ELSEVIER

European Journal of Radiology 26 (1998) 297–303

EJR
EUROPEAN JOURNAL OF RADIOLOGY

Can the IVIM model be used for renal perfusion imaging?

M.F. Müller [a,*], P.V. Prasad [b], R.R. Edelman [b]

[a] *Department of Radiology, University of Bern, Inselspital, Freiburgstrasse 4, CH-3010 Bern, Switzerland*
[b] *Department of Radiology, Beth Israel Hospital and Harvard Medical School, Boston, MA, USA*

Received 21 October 1996; received in revised form 10 January 1997; accepted 13 January 1997

Abstract

Objective: Renal perfusion imaging may provide information about the hemodynamic significance of a renal artery stenosis and could improve noninvasive characterization when combined with angiography. It was proposed previously that diffusion sequences could provide useful perfusion indices based on the intravoxel incoherent motion (IVIM) model. Owing to motion artifacts, diffusion imaging has been restricted to relatively immobile organs like the brain. With the availability of single-shot echo-planar imaging (EPI) our purpose was to evaluate the IVIM model in renal perfusion. *Methods and material:* Eight volunteers underwent diffusion-sensitive magnetic resonance (MR) imaging of the kidneys using a spin echo (SE) EPI sequence. The diffusion coefficients determined by a linear regression analysis and fits to the IVIM function were calculated. *Results and conclusion:* Our preliminary experience does not support the possibility of obtaining perfusion information using the IVIM model in the kidneys.

Keywords: Intravoxel incoherent motion; Magnetic resonance imaging; Kidney; Perfusion; Kidney diffusion

1. Introduction

Arterial hypertension is a significant health problem [1]. In less than 5% the cause is a stenosis of a renal artery [2]. Renal artery stenosis (RAS) is frequently found incidentally in normotensive individuals and may be etiologically unrelated to coexistent hypertension. Only when correction of the stenosis results in lowered blood pressure the term renovascular hypertension can be applied. Detection of renovascular disease has become increasingly important because effective treatment either by percutaneous transluminal angioplasty or surgical revascularization is available [3]. However, no cost-effective screening method with low risk currently exists. The currently accepted 'gold standard' for detection of RAS is X-ray arteriography [4,5], which is invasive, involves injection of iodinated contrast material and exposure to ionizing radiation. Moreover, this test does not indicate the hemodynamic significance of the stenosis. Traditional techniques to assess renal function include intravenous urography [6], peripheral and renal vein renin sampling [7], and nuclear medicine [8–10]. Newer diagnostic modalities to assess RAS include intravenous digital subtraction angiography [11–15], Doppler ultrasonography [16–18], captopril renography [19–23], computed tomography angiography [24,25], and magnetic resonance (MR) imaging. The optimal imaging method for this important diagnosis is not yet certain.

There are several MR angiographic techniques that show promise in the noninvasive evaluation of renovascular hypertension [26–33]. In addition, renal perfusion information might indicate the hemodynamic significance of the RAS thus improving its diagnostic accuracy. Of particular interest is a perfusion imaging technique that obviates the need for an exogenous contrast agent. One technique relying on an endogenous contrast mechanism was based on diffusion imaging techniques and is referred to as the intravoxel

* Corresponding author. Tel.: +41 31 16322435; fax: +41 31 3822503; e-mail: mueller@insel.unibe.ch

0720-048X/98/$19.00
PII S0720-048X(97)01161-3

incoherent motion (IVIM) model [34]. Since this technique could potentially provide perfusion information in addition to a measure of the molecular diffusion coefficient which has its own significance in the evaluation of ischemia [35], we looked into the possibility of applying the IVIM model to the kidneys.

1.1. The IVIM model

Application of MR to measure molecular diffusion has been known since its early development [36,37]. In biological systems, molecular diffusion is influenced by both microstructure and microdynamics (including flow through microvasculature, exchange and transport between different compartments) [38]. In practice, tissue could be thought to be made of primarily two compartments, intra- and extracellular, and recent data suggest that the exchange between these compartments is fast with respect to diffusion times of 20 ms [38]. In addition, phenomena such as microcirculation involving flow through randomly oriented channels influence in vivo tissue diffusion measurements. This realization led to the possibility of obtaining information about regional microvasculature blood flow using diffusion-type MR measurements. There have been two different approaches proposed to evaluate perfusion based on this idea. Both models assume microvasculature to be made up of several straight segments that change their orientation in a random fashion. One approach assumed that over the measurement time, typically tens of milliseconds, the perfusing spins stay within a linear segment of the capillary and thus could be rephased on even echoes [39,40]. The other approach views microcirculation as a pseudo-diffusion process (intravoxel incoherent motion). This model assumes that when observing at a macroscopical scale, microcirculation appears as a random walk process because spins change their direction during the measurement time at least once. These approaches rely on anatomical and physiological data from different sources in literature about distribution of sizes and velocities associated with the capillaries in the brain [41]. Preliminary data using either approach suggested the possibility of obtaining perfusion information through MR techniques relying on motion sensitivity.

Even though the term IVIM in general includes any type of motion that may contribute to the signal attenuation in a diffusion weighted sequence, the IVIM model [34] assumes that only microcirculation is a major contributor in addition to molecular diffusion. Next it is assumed that D^*, the diffusion coefficient associated with the microcirculation, is at least an order of magnitude larger compared to molecular diffusion coefficient $D_{\text{molecular}}$. Further, it is assumed there is negligible exchange between the vascular and extravascular compartments during the measurement interval. Under these restrictive assumptions, a biexponential signal decay as a function of the gradient sensitivity factor-b is expected [34]. From such a biexponential relationship it was then shown that potentially useful perfusion indices may be derived by assuming the following equation to describe the signal decay [34]:

$$I = I_0(f\exp(-b[D^* + \mathrm{D}_{\text{molecular}}]) + (1-f)\exp(-b\mathrm{D}_{\text{molecular}})) \quad (1)$$

where

- I is the measured signal intensity with a gradient sensitivity factor b.
- I_0 is the measured signal intensity with a gradient sensitivity factor $b = 0$.
- $D_{\text{molecular}}$ is the molecular diffusion coefficient D^* is assumed to be the pseudo-diffusion coefficient associated with microvascular flow. Even though considered as a perfusion index, this is not a 'real' parameter and cannot be measured in any other way.
- f is the volume fraction of microvasculature within the voxel and may be used as a perfusion index. When $f = 0$ or 1, the expression reduces to a single exponential form; if $f = 0$, $D_{\text{measured}} = D_{\text{molecular}}$ and if $f = 1$, $D_{\text{measured}} = D^* + D_{\text{molecular}}$.

Over the years, it has not been possible to reproduce the initial claims of deriving perfusion indices using the IVIM model in the brain [42]. This can be partially attributed to the small flow fraction associated with the brain. On the other hand, the kidney is the best perfused organ receiving about 25% of the cardiac output even though the organ mass is less than 1% of the total body mass [43] and is associated with a total (micro + macro) vascular density on the order of 20% by volume [44]. Thus, we hoped to make observations that would allow extraction of perfusion information from different diffusion weighted images in the kidney.

2. Subjects and methods

The subjects consisted of eight healthy human volunteers. All examinations were performed using a 1.5-T whole body imager (Siemens Medical Systems, Erlangen, Germany) with echo-planar imaging (EPI) capabilities. A cirularly polarized 18 cm flat surface coil positioned posteriorly was used for signal reception in all the studies.

A spin-echo (SE) EPI sequence with the following diffusion imaging parameters was used: diffusion gradient duration $\delta = 10$ ms, separation between the diffusion gradient pulses $\Delta = 28$ ms, TE = 60 ms, FOV = 300 mm × 300 mm, matrix = 64 × 128, slice thickness = 7 mm, and number of acquisitions = 1. The diffusion gradient pulses were applied along the slice

select direction with a maximum gradient amplitude of 28 mT/m. Sets of five images with different b-values were acquired at 3 second intervals within a breath hold which lasted for 15 s. In total, images with ten different b-values were acquired. Each image set was repeated three or four times in separate breath holds and the data was combined for analysis. The b-values for pairs of breath holds were interleaved, e.g. 103.9, 58.4, 26.0, 6.5, 1.6 in one breath hold and 141.4, 79.5, 40.6, 14.6, 1.6 s/mm^2 in another breath hold. The range of b values was chosen to be similar to those used by Turner et al. [45]. The descending order of the b-values within a breath hold was chosen to minimize sensitivity to respiratory motion that might occur towards the end of the breath hold period.

As a control, diffusion coefficients were measured using water and agar gel phantoms (Fig. 1).

2.1. Image and data analysis

The diffusion coeffficients were determined by a linear regression analysis of the ln(signal intensity) versus gradient factor (b). This analysis was performed by using regions of interest (ROI) over the kidney.

Fits to the IVIM function given by Eq. (1) were calculated.

3. Results

For validation purposes, diffusion coefficients were measured at room temperature (20°C) with the SE EPI diffusion pulse sequence in a phantom consisting of water and agar gel samples. The measured values as shown in Fig. 1 agreed very well with each other and with those previously reported in literature [46,47].

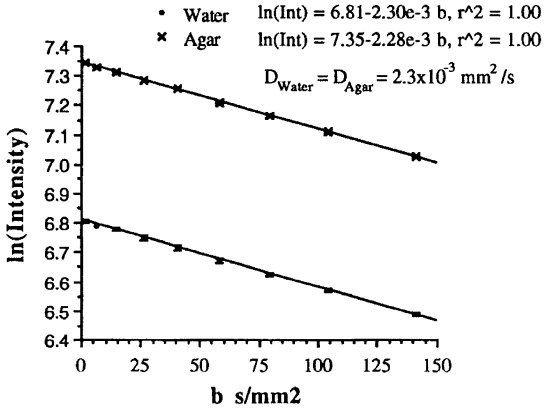

Fig. 1. Diffusion coeffficient calculation at room temperature using region of interest analysis on phantoms comprising of bottles filled with water and 3% agar, respectively. The measured diffusion coefficient given by the slope of the ln(intensity) versus b is $2.30 \times 10-3$ mm^2/s for water and $2.28 \times 10-3$ mm^2/s for agar.

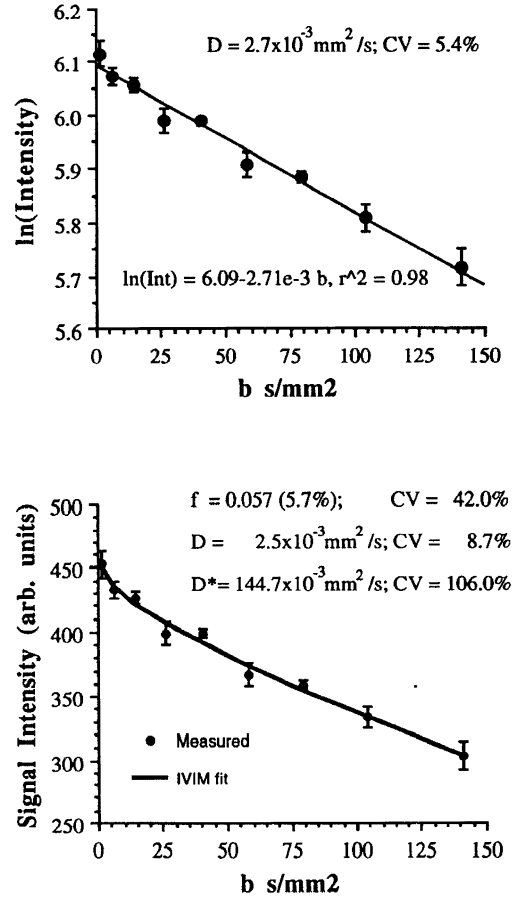

Fig. 2. (a) and (b) Diffusion coefficient calculation using ROI analysis on the right kidney. Since there was no significant contrast between cortex and medulla, no attempt was made to separate them. The data shown are mean ± S.D. of four repetitions. The diffusion coeffficient was estimated in two different ways as shown in (a) and (b). In (a) the ln(intensity) versus b data was fit to a straight line and D was estimated by the slope of the fitted line. In (b) the measured intensity versus b data was fit to the IVIM function. The fit parameters ware shown in the plot. Along with the parameter estimates the coefficient of variance (CV = standard error in the parameter estimate/parameter estimate) is shown for each parameter. Note that CV for D with either fit is relatively small and comparable, while CV for D^* and f is much smaller.

In the human volunteers no significant contrast between renal cortex and medulla was observed. Fig. 2 shows the ROI data obtained from a set of images. Each sequence was repeated four times for averaging purpose. The linear regression (Fig. 2 of the ln(intensity) versus b gave an r^2 value of 0.95 or better for all our data fits to the IVIM function given by Eq. (1) (Fig. 2b) were performed also. The mean ± S.D., averaged over the eight subjects studied, of $D^{\text{sinlge exp}}_{\text{measured}}$ (2.74 ± 0.24) and $D^{\text{biexp}}_{\text{measured}}$ (2.66 ± 0.57) were comparable. But estimates using the IVIM function resulted in larger coefficient variance (CV = standard error in the parameter estimate/parameter estimate) compared to the ln-linear fit. Also, no consistent value for f was

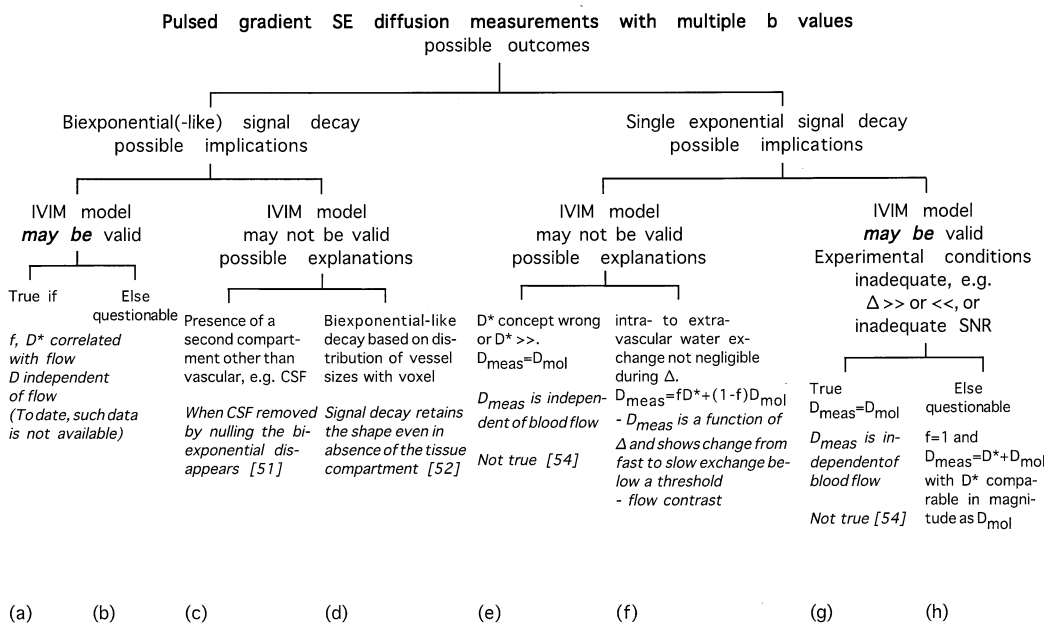

Fig. 3. Chart showing the possible outcomes of a pulsed gradient diffusion experiment with several b values. Also shown are the possible implications, explanations and supporting experimental evidence necessary for each outcome. Our data seem to support outcome h. Legends: Bold italics are used to place stress on 'may be'; plain italics are experimental data that will support the case. Unequivocal support for the IVIM model requires experimental data shown under (a). Alternate interpretations for biexponential signal decay have been previously put forth (c) and (d). If biexponential signal decay was not observed, (e) or (g) was assumed previously. But our data suggest outcomes (f) or (h).

obtained with the biexponential fit with values ranging all the way from 0 to 1 resulting in a means $\pm$ S.D. of 0.33 ± 0.42. The measured diffusion coefficients in the kidneys were significantly higher compared to any other abdominal organ previously reported [48].

4. Discussion

Our discussion starts with a consideration of possible outcomes of a spin echo diffusion experiment. Then we will provide arguments based on our results reported here and on previous publications to investigate the validity of the IVIM model to the study of renal perfusion. For the sake of clarity we (re-)define the following terms:

$D_{\text{molecular}}$ refers to the true molecular diffusion coefficient. This is a characteristic parameter that depends on the microscopic structural makeup of the tissue and can be assumed not to vary with transient and acute (< 10 min) physiological changes. It has been shown that ischemic insults do influence $D_{\text{molecular}}$ but it reflects true microscopic structural changes rather than direct effects of perfusion.

$D^{\text{single exp}}_{\text{measured}}$ is the estimate of in vivo $D_{\text{molecular}}$ obtained from a ln-linear fit.

$D^{\text{biexp}}_{\text{measured}}$ is the estimate of in vivo $D_{\text{molecular}}$ obtained from a biexponential measured fit.

Since we have found $D^{\text{single exp}}_{\text{measured}} \approx D^{\text{biexp}}_{\text{measured}}$ we will use D_{measured} to refer measured measured estimate of $D_{\text{molecular}}$ irrespective of the estimation method used. In phantoms and ex vivo samples, $D_{\text{measured}} = D_{\text{molecular}}$. This may (and was found) not to be case with in vivo measurements. D_{measured} is being used in place of the term apparent diffusion coefficient (ADC) used in our previous publications [48,49].

If one were to consider the possible outcomes of a pulse gradient SE diffusion experiment, the chart in Fig. 3 could be compiled. This chart includes the possible outcomes, their implications and possible explanations. Also included are any experimental data needed to support each particular case.

In order to prove the validity of the IVIM model unequivocally, it is necessary to demonstrate a biexponential signal decay, to show that the derived parameters can be obtained reproducibly, and that they behave consistently with the expectations of the model (f and D^* correlated with blood flow). While the proponents of the model have shown some evidence for the biexponential decay in the kidneys ($n = 1$) [45], no correlation between the estimated parameters and blood flow was included. Another study [50] showed correlation between D_{measured} and renal blood flow, but did not explicitly prove the existence of a biexponential decay owing to technical limitations. Here it is important to realize that the presence of a biexponential decay owing to technical limitations. Here it is important to realize that the presence of a biexpinential or biexponential-like signal decay could be explained also by the presence of a non-vascular compartment (e.g. CSF [51])

within the imaging voxel or by an alternate perspective recently proposed by Henkelman et al. [52] which assumes a fractual model for the vasculature. Thus the presence of a biexponential-like signal decay by itself does not support the validity of the IVIM model. This is especially important in the light of a recent report that demonstrates a biexponential-like signal decay obtained even in the absence of the extravaxcular compartment [53].

On the other hand, absence of biexponential decay does not necessarily imply that the IVIM model is invalid. The experimental conditions may be the limiting factor for not observing the biexponential decay (e.g. diffusion time Δ too small or too long). If that is the case, then according to the underlying assumptions of the IVIM model, $D_{\text{measured}} = D_{\text{molecular}}$ and thus should be independent of blood flow or any other physiological manipulation.

In all our data we do not observe any obvious biexponential signal decay. Both single- and biexponential fits yield similar D_{measured} which is consistently much higher than those in other abdominal organs like liver or spleen [48].

Our previous studies have shown that D_{measured} in the kidneys varies with blood flow [54]. Even though those observations were made using a different sequence (STEAM-EPI), they are still pertinent to this discussion. The major relevant difference between the SE and STEAM diffusion sequences is Δ value (28 ms for the SE and 770 ms for the STEAM diffusion sequence). A diffusion time Δ of 770 ms could be argued to be too long for flowing spins to contribute to the observed signal intensity. This would only imply that we should observe a single exponential decay. Hence outcomes (e)–(h) in Fig. 3 are still relevant for our discussion. Using the Spearman R analysis on the pooled data obtained with an unilateral progressive renal artery stenosis model in pigs ($n = 7$) [54], we found a very good correlation of D_{measured} in the kidney supplied by the stenosed vessel ($R = 0.88$, $P < 0.001$, $n = 19$) and no correlation of D_{measured} in the contralateral kidney ($R = 0.28$, $P = 0.24$, $n = 19$) with blood flow. The stenosis was created using balloon occluders placed around the renal artery and inflating them to different levels. Diffusion measurements were obtained within 5 min following inflation of the occluder. In two animals where the measurements were made, the post mortem (again within 5 min) D_{measured} for both kidneys were very similar to the value obtained with full occlusion in the affected kidney. Interestingly this value seems to be very similar to the live in vivo D_{measured} values obtained in organs like the liver or spleen [48] (probably implying $D_{\text{measured}} \rightarrow D_{\text{molecular}}$ when blood flow is completely shut off). This means in vivo renal $D_{\text{measured}} \neq D_{\text{molecular}}$. Powers et al. [50] have also observed dependence of D_{measured} on the renal blood flow.

From our observations (anomalously large D_{measured} value in the normal functioning kidney, absence of biexponential signal decay and variation of D_{measured} with blood flow), we can see that outcomes (f) or (h) in Fig. 3 are most appropriate to describe our data. Outcome (h) can be supported only by process of elimination, i.e. by eliminating all other outcomes. To support outcome (f), one needs to perform diffusion measurements with variable Δ and look for a change from single exponential (fast exchange) to biexponential (slow exchange) signal decay with decreasing Δ. If our data is any indication, Δ needs to be much smaller than 28 ms in order to be able to detect a biexponential signal decay. This requires much stronger gradient amplitudes than are available to us and hence beyond the scope of this study. As pointed out earlier, recent data suggest that intra- to extracellular exchange may be fast with respect to $\Delta = 20$ ms [55]. It is then conceivable that intra- and extravascular exchange would be similarly fast or even faster. If we assume intra- to extravascular exchange is fast with respect to Δ, then we could rewrite Eq. (1) as [55]

$$I = I_0(\exp[-b(f[D^* + \mathrm{D}_{\text{molecular}}] + [1-f]\mathrm{D}_{\text{molecular}})]) \quad (2)$$

For the sake of curiosity, we fit the observed signal decay to Eq. (2) and obtained the following mean $\pm$ S.D. over all eight subjects: f (microvascular flow fraction) $= 8.9 \pm 0.5\%$, $D_{\text{measured}} = 1.25 \pm 0.13 \times 10^{-3}$ mm^2/s, and $D^* = 17.75 \pm 1.04 \times 10^{-3}$ mm^2/s. The degree of intersubject consistency in all the fit parameters and the realistic numerical values of at least f and D_{measured} seem to add credence to outcome (f). But more thorough studies are necessary to validate this.

Even though D_{meaured} is correlated with blood flow, it is evident that we do not observe any direct effect of perfusion on D_{measured} because the corticomedullary contrast does not behave consistent with the relative regional blood flow. The data from Powers et al. [50] also suggested a lack of significant cortico-medullary difference. It is well known that cortical blood flow is several times higher compared to the medulla and the vascular architecture in the cortex is more randomly oriented compared to the medulla [56]. This argument would favor outcome (h), since (f) would expect a significant higher D_{measured} value in the cortex compared to the medulla based on differences in regional blood flow. If that would be the case, what do D_{measured} and f and D^* reflect? Since renal function is tightly coupled to the total renal blood flow [57], D_{measured} may be sensitive to renal function rather than being directly sensitive to regional renal blood flow. This is also supported by the fact that D_{measured} varies with the hydration state and with ureteral obstruction [54]. Since kidney function involves several unique transport mechanisms, it could be expected that they could influence

the microscopic water mobilities which in turn would influence the $D_{measured}$ values. The parameter f now assumes a value of 1 and means that the tissue behaves as a single well mixed compartment. D^* again does not have a physical interpretation, it is just accounts for the difference between the $D_{measured}$ and $D_{molecular}$ values.

5. Conclusions

No clear evidence for a biexponential signal decay was observed in the kidneys to support the IVIM model. But the renal dmeasured values were much higher than those measured in any other tissues and seem to be sensitive to renal blood flow. We feel the observed dependence of renal D measured values on renal blood flow may be due to flow dependent kidney function which involves several unique transport mechanisms. Further studies are necessary to fully understand the mechanisms influencing renal diffusion measurements and any possible significance of such measurements.

References

[1] Subcommittee on definition and prevalence of the 1984 Joint National Committee. Hypertension prevalence and the status of awareness, treatment, and control in the US (final report). Hypertension 1985; 7: 457–468.
[2] Dollery CT. Arterial hypertension. In: Wyngaarden JB, Smith LH, ed. Cecil textbook of medicine. 17 edn. Philadelphia: W.B. Saunders 1985; 1: 266–280.
[3] Hunt JC, Strong CG. Renovascular hypertesion: mechanisms, natural history, and treatment. Am J Cardiol 1973; 32: 562–574.
[4] Scott JA, Rake FE, Becker GJ. Angiographic assessment of renal artery pathology. AJR 1983; 141: 1299–1303.
[5] Bookstein JJ. Appraisal of arteriography in estimating the hemodynamic significance of renal arterystenosis. Invest Radiol 1966; 1: 281–294.
[6] Maxwell MH, Gonick HC, Wiita R, Kaufman JJ. Use of the rapid sequene intra-venous pyelogram in the diagnosis of renovascular hypertension. N Engl J Med 1964; 270: 213–220.
[7] Lüscher TF, Vetter H, Studer A, et al. Renal venous renin activity in various forms of curable renal hypertension. Clin Nephrol 1981; 16: 314–320.
[8] Sostre S, Osman M, Szabo Z. Estimating renal function from the visual analysis of Tc-99m DTPA images. Clin Nucl Med 1993; 18: 281–285.
[9] Higa T, Nakatsu M.A. comparision of methods in measurement of effective renal plasma flow and glomerular filtration rate in clinical practice. Clin Nucl Med 1993; 18: 877–883.
[10] Rabito CA, Moore RH, Bougas C, Dragotakes SC. Noninvasive, real-time monitoring of renal function: the ambulatory renal monitor. J Nucl Med 1993; 34: 199–207.
[11] Hillman BJ, Ovitt TW, Nudelman S. Digital video subtraction angiography of renal vascular abnormalities. Radiology 1981; 139: 277–280.
[12] Buonocore E, Meaney TF, Borkowsky GP, Pavlicek MS, Gallagher J. Digital subtraction angiography of the aorta and the renal arteries. Radiology 1981; 139: 28 1–286.
[13] Pistolesi GF, Maso R, Fllosto L. Venous digital subtraction angiography in the evaluation of renovascular hypertension. Eur J Radiol 1985; 5: 120–124.
[14] Wilms GE, Baert AL, Staessen JA, Amery AK. Renal artery stenosis: evaluation with intravenous digital subtraction angiography. Radiology 1986; 160: 713–715.
[15] Dunnick NR, Svetkey LP, Cohan RH. Intravenous digital subtraction renal angiography use in screening for renovascular hypertension. Radiology 1989; 171: 219–222.
[16] Handa N, Fukunaga R, Etani H, Yoneda S, Kimura K, Kamada T. Efficacy of echo-Doppler examination for the evaluation of renovascular disease. Ultrasound Med Biol 1988; 14: 1–5.
[17] Taylor DC, Kettler MD, Monetta GL. Duplex-ultrasound scanning the diagnosis of renal artery stenosis: a prospective evaluation. J Vasc Surg 1988; 7: 363–369.
[18] Middleton WD. Doppler US evaluation of renal artery stenosis: past, present, and future. Radiology 1992; 184: 307–308.
[19] Blyth WB. Captopril and renal alltoregulation. N Engl J Med 1983; 308: 390–391.
[20] Fommei E, Ghione S, Palla L. Renal scintigraphic captopril test in the diagnosis of renovascular hypertension. Hypertension 1987; 10: 212–220.
[21] Fanti S, Dondi M, Barozzi L, Levorato M, Monetti N. Detection of renal artery stenosis by means of Captopril renal scintigraphy in patients with multiple renal arteries. Clin Nucl Med 1992; 17: 849–852.
[22] Datseris IE, Momanji JB, Brown EA. Captopril renal scintigraphy in patients with hypertension and chronic renal failure. J Nucl Med 1994; 35: 251–254.
[23] Shamlou EK, Drane WE, Hawkins IF, Fennell III RS. Captopril renography and the hypertensive renal transplantation patient: a predictive test of therapeutic outcome. Radiology 1994; 190: 153–159.
[24] Galanski M, Prokop M, Chavan A, Schaefer CM, Jandeleit K, Nischelsky JE. Renal arterial stenoses: spiral CT angiography. Radiology 1993; 189: 185–192.
[25] Rubin GD, Dake MD, Napel S. Spiral CT of renal artery stenosis: comparison of three-dimensional rendering techniques. Radiology 1994; 190: 181–189.
[26] Kim D, Edelman RR, Kent KC, Porter DH, Skillman JJ. Abdominal aorta and renal artery stenosis: evaluation with MR angiography. Radiology 1990; 174: 727–731.
[27] Debatin JF, Spritzer CE, Grist TM. Imaging of the renal arteries: value of MR angiography. AJR 1991; 157(5): 981–990.
[28] Yucel EK. Magnetic resonance angiography of the lower extremity and renal arteries. Sem Ultrasound, CT, and MRI 1992; 13: 291–302.
[29] Loubeyre P, Revel D, Garcia P. Screening patients for renal artery stenosis: value of three-dimensional time-of-flight MR angiography. AJR 1994; 162: 847–852.
[30] Debatin JF, Ting RH, Wegmuller H. Renal artery blood flow: quantitation with phase-contrast MR imaging with and without breath holding. Radiology 1994; 190 (2): 371–378.
[31] Edelman RR, Siewert B, Adamis M, Gaa J, Laub G, Wielopolski P. Signal targeting with alternating radiofrequency (STAR) sequences: application to MR angiography. Magn Reson Med. 1994; 31: 233–238.
[32] Prasad PV, Kaiser A, Kim D. Noninvasive characterization of renal artery stenosis using a combination of SI AR angiography and EPISTAR perfusion imaging. Society of Magnetic Resonance and European Society for Magnetic Resonance in Medicine and Biology. Nice, France, 1995; 413.
[33] Snidow JJ, Johnson MS, Harris VJ. Three-dimensional gadolinium-enhanced MR angiography for aortoiliac inflow assessment plus renal arteryscreening in asingle breath hold. Radiology 1996; 198: 725–732.

[34] Le Bihan D, Breton E, Lallemand D, Aubin ML, Vignaud J, Laval-Jeantet M. Separation of diffusion and perfusion in intravoxel incoherent motion MR imaging. Radiology 1988; 168 (2): 497–505.
[35] Moseley ME, Kucharczyk J, Mintorovitch J. Diffusion-weighted MR imaging of acute stroke: correlation with T2-weighted and magnetic susceptibility-enhanced MR imaging in cats. Ajnr Am J Neuroradiol 1990; 11 (3): 423–9.
[36] Carr HY, Purcell EM. Effects of diffusion on free precession in nuclear magnetic resonance experiments. Phys Rev 1954; 94: 630–635.
[37] Steijskal EO, Tanner JE. Spin diffusion measurements: spin echoes in the presence of a time-dependent field gradient. J Chem Phys 1965; 42: 288–292.
[38] van Gelderen P, de Vleeschouwer MHM, DesPres D, Pekar J, Zijl PCM, Moonen CTW. Water diffusion in acute stroke. Magn Reson Med 1994; 31: 154–163.
[39] Ahn CB, Lee SY, Nalcioglu 0, Cho ZH. The effects of random directional distributed flow in nuclear magnetic resonance imaging. Med Phys 1987; 14 (1): 43–8.
[40] Young IR, Hall AS, Bryant DJ. Assessment of brain perfusion with MR imaging. J Comput Assist Tomogr 1988; 12: 721–727.
[41] Pavlik G, Rackl A, Bing RJ. Quantitative capillary tomography and blood flow in the cerebral cortex of cats: an in vivo microscopic study. Brain Res 1981; 208: 35–38.
[42] King MD, van BN, Busza AL, Houseman J, Williams SR, Gadian DG. Perfusion and diffusion MR imaging. Magn Reson Med 1992; 24 (2): 288–301.
[43] Harth O. Nierenfunktion. In: Schmidt RF, Thews G, ed. Physiologie des Menschen. 20th edn. Berlin, New York: Springer-Verlag, 1980: 668–702.
[44] Man RotTGoR. In: ICRP Publication. Oxford: Pergamon Press, 1975; 23: 176.
[45] Turner R, Le Bihan D, Maier J, Vavrek R, Baich J. Echo-planar IVIM imaging of the body application to kidney. Proceedings of the Society of Magnetic Resonance in Medicine. Ninth Annual Scientific Meeting. New York: 1990, 1136.
[46] Wesbey GE, Moseley ME, Ehman RL. Translational molecular selfdiffusion in magnetic resonance imaging II. Measurement of the selfdiffusion coefficient. Invest Radiol 1984; 19 (6): 491–8.
[47] Lorenz CH, D.R. P, Puffer DB, Price RR. Magnetic resonance diffusion/perfusion phantom experiments. Magn Reson Med 1991; 19: 254–260.
[48] Muller MF, Prasad PV, Siewert B, Nissenbaum MA, Raptopoulos V, Edelman RR. Abdominal diffusion mapping with use of a whole-body echoplanar system. Radiology 1994; 190: 475–478.
[49] Muller MF, Prasad PV, Siewert B, Edelman RR. In vivo echoplanar diffusion mapping of the kidney. First Meeting of the Society of Magnetic Resonance (SMR). Dallas, USA: J. Magn Reson Imaging, 1994; 97.
[50] Powers TA, Lorenz CH, Holburn GE, Price RR. Renal artery stenosis: In vivo perfusion MR imaging. Radiology 1991; 178: 543–548.
[51] Kwong KK, McKinstry RC, Chien D. CSF suppressed quantitative single-shot diffusion imaging. Proceedings of the Society of Magnetic Resonance in Medicine. Tenth Annual Scientific Meeting. San Francisco: 1991, 215.
[52] Henkelman RM, Neil JJ, Xiang QS. A quantitative interpretation of IVIM measurements of vascular perfusion in the rat brain. Magn Reson Med 1994; 32: 464–469.
[53] Neil JJ, Ackerman JJH. Detection of pseudodiffusion in rat brain following blood substitution with perflurocarbon. J Magn Reson 1992; 97: 194–197.
[54] Muller MF, Prasad PV, Bimmler D, Kaiser A, Edelman RR. Functional imaging of the kidney by means of measurement of the apparent diffusion coefficient. Radiology 1994; 193:71 1–715.
[55] van Gelderen P, de Vleeschouwer MHM, DesPres D, Pekar J, van Zijl PCM, Moonen CTW. Water diffusion and acute stroke. Magn Reson Med 1994; 31(1): 154–163.
[56] Ulfendahl HR, Wolgast M. Renal circulation and lymphatics. In: Seldin DW, Giebisch G, ed. The Kidney Physiology and Pathophysiology. 2nd edn. New York: Raven Press 1992: 2; 1017–1047.
[57] Kriz W, Kaissling B. Structural organization of the mammalian kidney. In: Seldin DW, Giebisch G, ed. The Kidney Physiology and Pathophysiology. 2nd edn. New York: Raven Press 1992; 1: 707–777.